Entangled two-photon source using biexciton emission of an asymmetric quantum dot in a cavity

T. M. Stace*
Cavendish Laboratory, University of Cambridge, Madingley Road, Cambridge CB3 0HE, United Kingdom

G. J. Milburn
DAMTP, University of Cambridge, Wilberforce Road, Cambridge CB3 OWA, United Kingdom
and Centre for Quantum Computer Technology, University of Queensland, St. Lucia, Queensland 4072, Australia

C. H. W. Barnes
Cavendish Laboratory, University of Cambridge, Madingley Road, Cambridge CB3 0HE, United Kingdom
(Received 9 September 2002; revised manuscript received 2 December 2002; published 28 February 2003)

A semiconductor based scheme has been proposed for generating entangled photon pairs from the radiative decay of an electrically pumped biexciton in a quantum dot. Symmetric dots produce polarization entanglement, but experimentally realized asymmetric dots produce photons entangled in both polarization and frequency. In this work, we investigate the possibility of erasing the ''which-path'' information contained in the frequencies of the photons produced by asymmetric quantum dots to recover polarization-entangled photons. We consider a biexciton with nondegenerate intermediate excitonic states in a leaky optical cavity with pairs of degenerate cavity modes close to the nondegenerate exciton transition frequencies. An open quantum system approach is used to compute the polarization entanglement of the two-photon state after it escapes from the cavity, measured by the visibility of two-photon interference fringes. We explicitly relate the two-photon visibility to the degree of the Bell-inequality violation, deriving a threshold at which Bell-inequality violations will be observed. Our results show that an ideal cavity will produce maximally polarization-entangled photon pairs, and even a nonideal cavity will produce partially entangled photon pairs capable of violating a Bell-inequality.

DOI: 10.1103/PhysRevB.67.085317 PACS number(s): 78.67.Hc, 12.20.Ds, 03.65.Yz, 42.50.Ct

I. INTRODUCTION

Recent proposals for quantum communication[1,2] and quantum information protocols[3] provide a significant incentive to develop practical single-photon sources and entangled two-photon sources. The first requirement for such sources is that the emission time of the photons be periodic with a precisely defined clock frequency. Exciton recombination in electrically or optically excited quantum dots is a candidate system for such sources. In this paper, we will discuss an entangled two-photon source based on recent experiments in self-assembled interface quantum dots.[4,5] A proposal for producing entangled photon pairs on demand based on biexciton emission from a quantum dot was recently presented by Benson *et al.*[6]

A pair of excitons confined in a quantum dot form a bound state known as a biexciton. The decay of the biexciton proceeds by consecutive single-electron-hole recombination processes. This is estabished experimentally by the temporal correlation of the biexciton emission and the exciton emission; time-resolved photoluminescence measurements show the exciton photon to be emitted *after* the biexciton photon.[5] A similar time-resolved study of the polarization of the emitted photons shows that there are two decay paths, and it has been shown that they are coherent with one another.[7] While the biexciton photon and the exciton photon emitted in each decay path have the same linear polarization, the polarization in different decay paths are orthogonal. If these decay paths were indistinguishable, then this would be a good candidate for an entangled two-photon source. Unfortunately small asymmetries in the physical geometry of the dots makes the two paths distinguishable, since the asymmetry of the dot breaks the degeneracy of an intermediate exciton level enabling the two paths to be distinguished by frequency. The effect of asymmetry on the spectrum of excitons in dots was observed experimentally in dots formed by monolayer fluctuations in a GaAs two-dimensional quantum well[8] and has been addressed theoretically.[9] It has also been observed experimentally in CdSe or ZnSe dots[10] and in self-assembled GaAs or InGaAs dots.[11] In Fig. 1(a), we indicate the possible decay paths from a single biexciton level through two nondegenerate exciton levels to the ground state of the dot. The first decay path corresponds to the emission of a biexciton photon with linear polarization in the x direction at frequency ω_1, followed by the emission of the exciton photon, with the same polarization, at frequency ω_2. In the second decay path, the biexciton emits a y polarized photon at frequency ω_3 followed by the exciton emission, also with y polarization, at frequency ω_4.

The state of the emitted photon pairs may then be written as

$$|\psi_1\rangle = (|\mathrm{x},\omega_1;\mathrm{x},\omega_2\rangle + |\mathrm{y},\omega_3;\mathrm{y},\omega_4\rangle)/\sqrt{2}, \qquad (1)$$

where the notation indicates the mode (polarization and frequency) occupied by each photon of the pair, $|\text{photon 1};\text{photon 2}\rangle$, with the order reflecting the order of emission. It has been established experimentally that the weights of the kets are equal.[11] In contrast, we wish to produce a state of the form

$$|\psi_2\rangle = |\mathrm{x},\omega_A;\mathrm{x},\omega_B\rangle + |\mathrm{y},\omega_A;\mathrm{y},\omega_B\rangle/\sqrt{2}, \qquad (2)$$

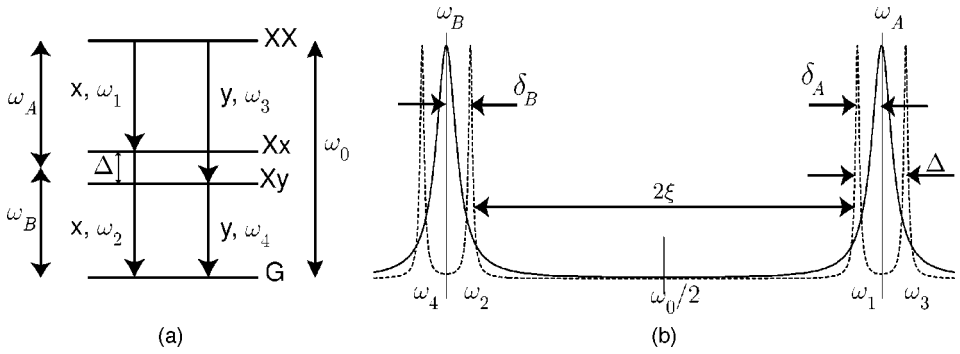

FIG. 1. (a) Energy-level diagram and available transitions for the quantum dot and cavity system. (b) Spectrum of exciton transitions (dotted line) and cavity modes (solid line) indicating the relevant frequencies for the interaction Hamiltonian.

and we call such a state polarization entangled, since the entanglement is only in the polarization degree of freedom. This is in contrast to the state given by Eq. (1) which is entangled in both polarization and frequency. The important difference between states $|\psi_1\rangle$ and $|\psi_2\rangle$ is that the second ket in $|\psi_2\rangle$ may be rotated into the first ket using linear optical elements such as half-wave plates (HWP) and polarizing beam splitters (PBS), and vice versa, whereas this is not possible for the two kets written in state $|\psi_1\rangle$. Thus, for instance, Bell-inequality measurements and two-photon interference experiments may be performed with realtive ease using $|\psi_1\rangle$ but not $|\psi_2\rangle$, and this translates to a technological setting in, for instance, quantum key distribution.

The problem of producing frequency-and-polarization entangled states akin to $|\psi_1\rangle$ has been considered for photon pairs produced by spontaneous parametric down-conversion in a nonlinear crystal.[12] In this case, photons are also entangled both in polarization and frequency, though the frequency entanglement is more complicated. The frequencies for the two emitted photons are constrained by energy conservation, so that their sum must be equal to the frequency of the absorbed pump photon. Since this single constraint does not determine the frequencies of the two emitted photons uniquely, each photon of the pair may be emitted over a wide range of frequencies determined by the spectrum of the pump pulse and the phase-matching requirement (which is an expression of momentum conservation). Thus, the photon pair is entangled in its frequency degree of freedom.

A resolution to this problem, presented and experimentally implemented in Ref. 12 is to pass the signal and idler beams back through the crystal, but with the polarizations rotated through $\pi/2$, with the result that the two ways in which the photons can be emitted with correlated polarization are not distinguished by frequency. This scheme in Ref. 12 does not directly translate to the case of biexcitonic emission, but we, nevertheless wish to remove the spectral dependence from the entanglement in state $|\psi_1\rangle$, so the objective of this paper is to present and analyze a proposal to accomplish this for the biexciton entangled photon source.

In this paper, we demonstrate that the frequency may be disentangled from the polarization by placing the dot in an external cavity with suitably chosen cavity-exciton coupling strengths and cavity mode frequencies. We will show that the external cavity can erase the ''which-path'' information contained in the frequency components of state $|\psi_1\rangle$. The external cavity is used to control both the spectral and spatial mode structures of the emitted photons to enable the entanglement to be demonstrated in an interferometer. A similar idea using waveguides for spontaneous parametric down-conversion has been proposed by Banaszek *et.al.*[13] We note that the original proposal for the two-photon source[6] includes the external cavity, but its presence is only to increase the outcoupling efficiency, and only a brief mention is made of its effect upon the spectral emission properties of the emitted photons.

The following part of this paper begins by defining a Hamiltonian for a four-level system interacting with optical cavity modes. A master equation is developed in Sec. III to deal with photons leaking from the cavity and into some measurement apparatus, as well as to account for decoherence events such as photon loss. In Sec. IV, we discuss some operational definitions to quantify the entanglement of the photons produced, such as two-photon visibility and Bell-inequality violations, with the aid of which we judge the efficacy of the cavity in restoring the polarization entanglement. We then provide some results in Secs. V and VI showing that an ideal cavity does establish maximally entangled photon pairs, and numerical results showing how sensitive the resulting state is to imperfections in the system parameters. We then provide some heuristic analytic results in the Discussion, which explain the numerical results, as well as comment on implications for experiments, and finally conclude the paper.

II. SYSTEM HAMILTONIAN

Figure 1(a) shows the energy levels and available dipole transitions for the biexciton-cavity system. The biexciton states given by $|XX\rangle$, $|X\mathsf{x}\rangle$ and $|X\mathsf{y}\rangle$ are the intermediate excitonic states in the x and y polarization decay paths respectively, and $|G\rangle$ is the dot ground state. The cavity is assumed to support pairs of degenerate x- and y-polarized modes at frequencies ω_A and ω_B. In our model, we do not include coupling between, for instance, the cavity mode $|\omega_A,\mathsf{x}\rangle$ and the transition $|G\rangle\leftrightarrow|X\mathsf{x}\rangle$ which is valid when assuming that the detuning between them is much larger than the cavity-exciton coupling strength, which is the case for this system. The system Hamiltonian $H_{\rm sys}$ under the rotating wave and dipole approximations[14,15] is then

$$\begin{aligned} H_{\rm sys} = {} & \omega_0|XX\rangle\langle XX| + \omega_2|X\mathsf{x}\rangle\langle X\mathsf{x}| + \omega_4|X\mathsf{y}\rangle\langle X\mathsf{y}| \\ & + \omega_A(\hat{n}_{\mathsf{x},\omega_A} + \hat{n}_{\mathsf{y},\omega_A}) + \omega_B(\hat{n}_{\mathsf{x},\omega_B} + \hat{n}_{\mathsf{y},\omega_B}) \\ & + \frac{i}{2}(q_1|X\mathsf{x}\rangle\langle XX|a^\dagger_{\mathsf{x},\omega_A} + q_2|\mathsf{G}\rangle\langle X\mathsf{x}|a^\dagger_{\mathsf{x},\omega_B} \\ & + q_3|X\mathsf{y}\rangle\langle XX|a^\dagger_{\mathsf{y},\omega_A} + q_4|\mathsf{G}\rangle\langle X\mathsf{y}|a^\dagger_{\mathsf{x},\omega_A} - \text{H.c.}), \end{aligned} \tag{3}$$

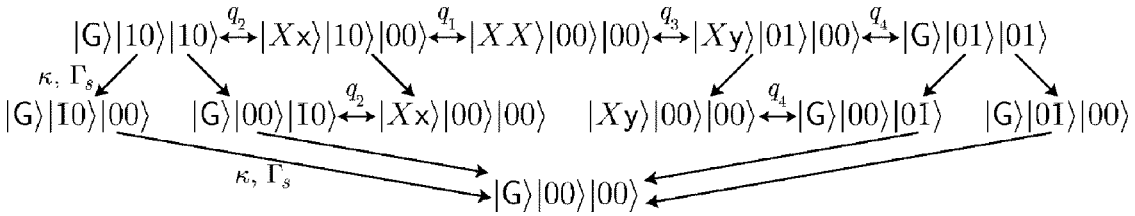

FIG. 2. The basis B for the evolution of the system along with transitions generated by the Hamiltonian H and cavity leakage. Coupling strengths between states are indicated. The top line of states spans the subspace of two excitations (i.e., exciton number plus photon number), the middle line spans the subspace of one excitation, and the single state on the last line spans the subspace of zero excitations.

where a_j and $\hat{n}_j = a_j^\dagger a_j$ are the photon annihilation operator and the photon number operator for mode j, respectively, and for convenience we take $\hbar = 1$. We transform to an interaction picture defined by $H_0 = (\omega_0/2)\hat{N}$, where

$$\hat{N} = 2|XX\rangle\langle XX| + |X\mathrm{x}\rangle\langle X\mathrm{x}| + |X\mathrm{y}\rangle\langle X\mathrm{y}| + \hat{n}_{\mathrm{x},\omega_A} + \hat{n}_{\mathrm{y},\omega_A} + \hat{n}_{\mathrm{x},\omega_B} + \hat{n}_{\mathrm{y},\omega_B} \tag{4}$$

is the number of excitations in the system. The interaction Hamiltonian, $H = e^{iH_0 t} H_{\mathrm{sys}} e^{-iH_0 t} - H_0$, is given by

$$\begin{aligned} H = &-\xi|X\mathrm{x}\rangle\langle X\mathrm{x}| - (\xi+\Delta)|X\mathrm{y}\rangle\langle X\mathrm{y}| \\ &+ (\xi+\delta_A)(\hat{n}_{\mathrm{x},\omega_A} + \hat{n}_{\mathrm{y},\omega_A}) - (\xi+\delta_B)(\hat{n}_{\mathrm{x},\omega_B} + \hat{n}_{\mathrm{y},\omega_B}) \\ &+ \frac{i}{2}(q_1|X\mathrm{x}\rangle\langle XX|a^\dagger_{\mathrm{x},\omega_A} + q_2|\mathrm{G}\rangle\langle X\mathrm{x}|a^\dagger_{\mathrm{x},\omega_B} + q_3|X\mathrm{y}\rangle \\ &\times\langle XX|a^\dagger_{\mathrm{y},\omega_A} + q_4|\mathrm{G}\rangle\langle X\mathrm{y}|a^\dagger_{\mathrm{x},\omega_A} - \mathrm{H.c.}), \end{aligned} \tag{5}$$

where $2\xi = \omega_1 - \omega_2$ is the biexciton shift, $\Delta = \omega_3 - \omega_1 = \omega_2 - \omega_4$ is the doublet splitting due to dot asymmetry, $\delta_A = \omega_A - \omega_1$ is the detuning between cavity mode A and transition frequency ω_1, and $\delta_B = \omega_2 - \omega_B$ is the detuning between transition frequency ω_2 and cavity mode B. These frequencies are shown schematically in Fig. 1(b).

We now define a ''balanced cavity'' to be one for which the two cavity modes fall directly in between each of the doublets ($\delta_A = \delta_B = \Delta/2$) and the exciton-cavity coupling constants are matched ($q_1 = q_3$ and $q_2 = q_4$). An ''unbalanced cavity'' is one for which $\delta_{A,B} \neq \Delta/2$, and ''unbalanced coupling'' means that $q_1 \neq q_3$ or $q_2 \neq q_4$). We will show later that a balanced cavity accomplishes the required which-path erasure.

The dynamics of states under the action of the time evolution operator, e^{-iHt}, generated by the Hamiltonian H is closed in the 12-dimensional space spanned by the basis B, which is shown in Fig. 2.

Finally, we assume that the initial state of the system is biexcitonic, $|\psi(0)\rangle = |XX\rangle|00\rangle|00\rangle$.

III. DERIVATION OF MASTER EQUATION

The theory of open quantum systems has been well studied (see e.g., Refs. 16 and 17), and we adopt this formalism to analyze the exciton-cavity system interacting with the external continuum modes and measurement devices outside the cavity.

Wiseman[16] gives an expression for the master equation for the conditional density matrix, ρ_c, for a single measurement channel using imperfect detectors, while Gardiner and Zoller[17] give a similar expression for many channels with perfect detection on each channel. Generalizing these results to an n-channel conditional master equation with arbitrary efficiency detectors on each channel results in the conditional master equation

$$\begin{aligned} d\rho_c = &-i[H,\rho_c]dt + \sum_{j=1}^{n}\left\{\left(\eta_j \mathrm{Tr}\{\mathcal{J}_j\rho_c\}\rho_c + (1-\eta_j)\mathcal{J}_j\rho_c \right.\right. \\ &\left.\left. - \frac{1}{2}(c_j^\dagger c_j\rho_c + \rho_c c_j^\dagger c_j)\right)dt + \left(\frac{\mathcal{J}_j\rho_c}{\mathrm{Tr}\{\mathcal{J}_j\rho_c\}} - \rho_c\right)dN_j\right\}, \end{aligned} \tag{6}$$

where H is the interaction Hamiltonian for the system, c_j is the system operator through which the system couples to channel j, $\mathcal{J}_j\rho_c \equiv c_j\rho_c c_j^\dagger$ is the jump operator for channel j, η_j is the detection efficiency of jump processes on channel j, and dN_j is the jump increment. For the case where $\eta_j = 1$ for all j, this equation reproduces the result in Gardiner and Zoller[17] [Sec. 11.3.8.d], and for $n = 1$ it reproduces the result of Wiseman[16] [Sec. 4.1.2].

For the biexciton decay, there are several baths with which the exciton-cavity system is coupled. First, the cavity modes decay at a rate κ in order to couple the photons generated in the emission process to the outside world. This decay mode is coupled to the four cavity modes, where the system coupling operators are $c_1 = \sqrt{\kappa}a_{\mathrm{x},\omega_A}$, $c_2 = \sqrt{\kappa}a_{\mathrm{y},\omega_A}$, $c_3 = \sqrt{\kappa}a_{\mathrm{x},\omega_B}$, and $c_4 = \sqrt{\kappa}a_{\mathrm{y},\omega_B}$. To quantify the effect of the cavity in erasing the frequency information, in what will follow, these channels are assumed to be perfectly detected, $\eta_1 = \cdots = \eta_4 = 1$.

Second, there may be a spontaneous emission into photon modes apart from those of the cavity. This decay channel couples via similar system operators, but with different decay rates, so that $c_5 = \sqrt{\Gamma_s}|X\mathrm{x}\rangle\langle XX|$, $c_6 = \sqrt{\Gamma_s}|X\mathrm{y}\rangle\langle XX|$, $c_7 = \sqrt{\Gamma_s}|\mathrm{G}\rangle\langle X\mathrm{x}|$, and $c_8 = \sqrt{\Gamma_s}|\mathrm{G}\rangle\langle X\mathrm{y}|$. These channels are considered to be inaccessible to an observer, so we set the detection efficiency to zero, $\eta_4 = \cdots = \eta_8 = 0$. For later sections, we will refer to these channels as ''leakage channels.''

Finally, we will add a phenomenological dephasing acting on the two exciton states $|X\mathrm{x}\rangle$ and $|X\mathrm{y}\rangle$. This is to simulate the effect of some unspecified bath (e.g., phonons) that is able to distinguish the intermediate excitonic state during the

decay process. The system operators to which this bath couples are assumed to be $c_9=\sqrt{\Gamma_d}|X\mathrm{x}\rangle\langle X\mathrm{x}|$, and $c_{10}=\sqrt{\Gamma_d}|X\mathrm{y}\rangle\langle X\mathrm{y}|$. Again, these channels are inaccessible to observer, so the detection efficiency is zero, $\eta_9=\eta_{10}=0$.

Since $\eta_j=0$ for channels five through ten, from Ref. 16 we have $E[dN_j(t)]=\eta_j\mathrm{Tr}\{\mathcal{J}_j\rho_c(t)\}dt=0$ for $j=5,\ldots,10$, and since $dN_j(t)$ is non-negative, $dN_j(t)=0$ for $j=5,\ldots,10$. In accordance with the assumptions regarding channel efficiencies made above, the conditional master equation between photon detections (i.e., $dN_j=0$, $j=1,\ldots,4$), becomes

$$\dot{\rho}_c=-i[H,\rho_c]+\sum_{j=1}^{4}\mathrm{Tr}\{\mathcal{J}_j\rho_c\}\rho_c+\sum_{j=5}^{10}\mathcal{J}_j\rho_c-\sum_{j=1}^{10}\frac{1}{2}(c_j^\dagger c_j\rho_c+\rho_c c_j^\dagger c_j). \tag{7}$$

The second term in this equation is nonlinear in ρ_c, reflecting the fact that the evolution is conditional on the system not emitting a photon. For computational purposes, we convert Eq. (7) into an equivalent linear equation for an unnormalized density matrix $\tilde{\rho}$ by defining $\rho_c(t)=f(t)\tilde{\rho}(t)$, where $f(t)$ is a scalar function to be determined. Substituting this into Eq. (7) gives

$$\dot{f}\tilde{\rho}+f\dot{\tilde{\rho}}=-if[H,\tilde{\rho}]+f^2\sum_{j=1}^{4}\mathrm{Tr}\{\mathcal{J}_j\tilde{\rho}\}\tilde{\rho}+f\sum_{j=5}^{10}\mathcal{J}_j\tilde{\rho}-f\sum_{j=1}^{10}\frac{1}{2}(c_j^\dagger c_j\tilde{\rho}+\tilde{\rho}c_j^\dagger c_j). \tag{8}$$

Collecting terms that are proportional to f and requiring that others vanish gives the linear, unnormalized semi-conditional (i.e., conditioned on only a subset, $j=1,\ldots,4$, of the channels) master equation

$$\dot{\tilde{\rho}}=-i[H,\tilde{\rho}]+\sum_{j=5}^{10}\mathcal{J}_j\tilde{\rho}-\sum_{j=1}^{10}\frac{1}{2}(c_j^\dagger c_j\tilde{\rho}+\tilde{\rho}c_j^\dagger c_j), \tag{9}$$

along with the constraint equation for f

$$\dot{f}\tilde{\rho}=f^2\sum_{j=1}^{4}\mathrm{Tr}\{\mathcal{J}_j\tilde{\rho}\}\tilde{\rho}. \tag{10}$$

This can be integrated to give $f=-(\int^t dt\,\Sigma_{j=1}^4\mathrm{Tr}\{\mathcal{J}_j\tilde{\rho}\})^{-1}$. Taking the trace of Eq. (9) gives $\mathrm{Tr}\{\dot{\tilde{\rho}}\}=-\Sigma_{j=1}^4\mathrm{Tr}\{\mathcal{J}_j\tilde{\rho}\}$, and so we see that $f=\mathrm{Tr}\{\tilde{\rho}\}^{-1}$, which is just the normalization condition for ρ_c, i.e., $\rho_c=\tilde{\rho}/\mathrm{Tr}\{\tilde{\rho}\}$ as required.

IV. QUANTIFYING TWO-PHOTON ENTANGLEMENT

We now develop a measure of the performance of the cavity in erasing which-path information. A polarization-entangled photon pair is an archetypal example of a two-qubit system. Such bipartite systems have been studied extensively,[1] and in particular, the entanglement of such pure bipartite systems is well quantified by the von Neumann entropy of one subsystem.

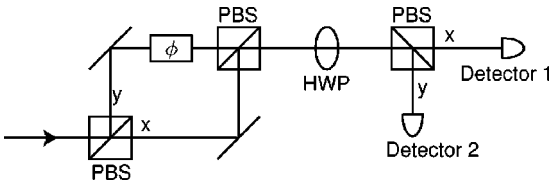

FIG. 3. Schematic of a polarization sensitive interferometer. A PBS splits the beam into x- and y-polarized paths and a relative phase ϕ is added to one path. The paths are recombined, and the polarizations are rotated by $\pi/4$ using HWP, then detected with polarization-sensitive single-photon detectors.

In the system we are concerned with, there is some subtlety, however, since although the system plus continuum evolves to a two-photon state, this is only determined once a measurement has been performed, observing both photons. Before the measurement, the system evolves in a much larger Hilbert space, so it is not entirely trivial to adapt measures such as entropy to the case of interest here, not least, because under certain circumstances, the photon pair is described by a mixed state. Instead, we use an operational measure—the visibility. This arises naturally by considering the result of two-photon coincidence counting at the output of a polarization-sensitive interferometer, depicted in Fig. 3, through which the photon pair is directed.

It is straightforward to show that a pure, entangled state of the form $|\mathrm{xx}\rangle+|\mathrm{yy}\rangle$ passing through such an interferometer with a ϕ phase shift (per photon) on one arm will exhibit interference fringes in the two-photon coincidence counts between the detectors, with the coincidence count rate proportional to $1-\cos(2\phi)$. The factor of 2 in the argument of the cosine is a direct manifestation of the two-particle nature of the state, and this has been observed experimentally.[18]

Conversely, neither a completely mixed state such as $|\mathrm{xx}\rangle\langle\mathrm{xx}|+|\mathrm{yy}\rangle\langle\mathrm{yy}|$ nor a pure, nonentangled state such as $|\mathrm{xx}\rangle$ will display interference fringes as ϕ is varied. It is intuitively clear from these two examples that the visibility of the interference fringes is an operational measure of both the purity and entanglement of the input two-photon state, and is dependent on the off-diagonal elements of the density matrix, which are zero for nonentangled or completely mixed states.

Interferometric methods for estimating entanglement have been discussed by Ekert and Horodecki.[19] They argue that d^2-1 separate types of interferometric experiment are required to estimate the entanglement of a pair of particles, d being the dimension of the Hilbert space for each particle. For the case of interest to us $d=2$, we expect that three parameters will be sufficient to place bounds on the entanglement of the photon pair. In fact, we assume that anticorrelated states such as $|\mathrm{xy}\rangle$ are never produced, which is roughly consistent with experimental observations showing that interexciton transitions are rare,[11] and so the number of experiments required is reduced to one. That is, we only need to measure a single visibility fringe in order to quantify the two-photon entanglement.

A. Interferometry

Quantitatively, we relate the output continuum field annihilation operators of the half-wave plate, $b'_{\mathrm{x},\omega}, b'_{\mathrm{y},\omega}$, to the interferometer input field operators, $b_{\mathrm{x},\omega}, b_{\mathrm{y},\omega}$, according to

$$\begin{bmatrix} b'_{\mathrm{x},\omega} \\ b'_{\mathrm{y},\omega} \end{bmatrix} = \frac{1}{\sqrt{2}} \begin{bmatrix} e^{i\phi} & 1 \\ -1 & e^{-i\phi} \end{bmatrix} \begin{bmatrix} b_{\mathrm{x},\omega} \\ b_{\mathrm{y},\omega} \end{bmatrix}. \tag{11}$$

We adopt the notation that a prime on an operator indicates that it is transformed consistently with Eq. (11), for example, $\hat{n}'_{\mathrm{x},\omega} = (b'_{\mathrm{x},\omega})^\dagger b'_{\mathrm{x},\omega}$.

The expectation of a two-photon coincidence measurement by detectors 1 and 2 will, in general, be given by the normally ordered (denoted by $:\cdots:$) two-time correlation function $\langle :\hat{n}'_{i,\omega_B}(t_B)\hat{n}'_{j,\omega_A}(t_A):\rangle_c$, where $i,j \in \{\mathrm{x},\mathrm{y}\}$.[16,17,20] The subscript c denotes the fact that the expectation is conditioned on the system having emitted zero photons in the interval $[0,\min\{t_A,t_B\}]$, and the ordering of the operators in the correlation function will depend on the ordering of t_A and t_B.

We may relate the cavity field output operators for the continuum mode l to the cavity input operators and the internal cavity operator according to $b_{\mathrm{out}}(l,t) - b_{\mathrm{in}}(l,t) = \sqrt{\kappa} a_l(t)$. We will also assume that the cavity input is the vacuum so $\langle b^\dagger_{\mathrm{in}}(l,t) b_{\mathrm{in}}(l,t')\rangle = 0$.[17] Thus, normally ordered expectations of continuum modes may be replaced by normal- and time-ordered expectations of internal cavity modes, multiplied by a suitable power of $\sqrt{\kappa}$. More detailed discussion of this point is given in Gardiner and Zoller.[17]

For example, the conditional expectation of detecting consecutive photons at detector 1 will be given by $\langle :\hat{n}'_{\mathrm{x},\omega_B}(t_B)\hat{n}'_{\mathrm{x},\omega_A}(t_A):\rangle_c$, and if $t_B > t_A$, then

$$\begin{aligned} \langle :\hat{n}'_{\mathrm{x},\omega_B}(t_B)\hat{n}'_{\mathrm{x},\omega_A}(t_A):\rangle_c &= \mathrm{Tr}\{\mathcal{J}'_{\mathrm{x},\omega_B}(t_B)\mathcal{T}(t_B,t_A) \\ &\quad \times \{\mathcal{J}'_{\mathrm{x},\omega_A}(t_A)\rho_c(t_A)\}\} \\ &= \kappa^2 \mathrm{Tr}\{(a'_{\mathrm{x},\omega_B})^\dagger a'_{\mathrm{x},\omega_B} \mathcal{T}(t_B,t_A) \\ &\quad \times \{a'_{\mathrm{x},\omega_A}\rho_c(t_A)(a'_{\mathrm{x},\omega_A})^\dagger\}\}, \end{aligned} \tag{12}$$

where $\mathcal{T}(t_B,t_A)$ is the time evolution operator, which evolves the system from time t_A to time t_B, and for open systems it is nonunitary.[17] Very similar expressions may be derived for the case where $t_B < t_A$.

B. Visibility

Since the transformed operators in Eq. (12) depend on ϕ according to Eq. (11), we see that the quantity $\langle :\hat{n}'_{\mathrm{x},\omega_B}(t_B)\hat{n}'_{\mathrm{x},\omega_A}(t):\rangle$ must also depend on ϕ. Many of the cross terms vanish, leaving the result

$$\langle :\hat{n}'_{\mathrm{x},\omega_B}(t_B)\hat{n}'_{\mathrm{x},\omega_A}(t_A):\rangle = \kappa^2(x + y + e^{2i\phi}z + e^{-2i\phi}z^*), \tag{13}$$

where

$$\begin{aligned} x &\equiv \langle :a^\dagger_{\mathrm{x},\omega_B} a_{\mathrm{x},\omega_B} a^\dagger_{\mathrm{x},\omega_A} a_{\mathrm{x},\omega_A}:\rangle \\ &= \mathrm{Tr}\{a^\dagger_{\mathrm{x},\omega_B} a_{\mathrm{x},\omega_B} \mathcal{T}\{a_{\mathrm{x},\omega_A}\rho_c a^\dagger_{\mathrm{x},\omega_A}\}\} \in [0,1], \\ y &\equiv \langle :a^\dagger_{\mathrm{y},\omega_B} a_{\mathrm{y},\omega_B} a^\dagger_{\mathrm{y},\omega_A} a_{\mathrm{y},\omega_A}:\rangle \\ &= \mathrm{Tr}\{a^\dagger_{\mathrm{y},\omega_B} a_{\mathrm{y},\omega_B} \mathcal{T}\{a_{\mathrm{y},\omega_A}\rho_c a^\dagger_{\mathrm{y},\omega_A}\}\} \in [0,1], \\ z &\equiv \langle :a^\dagger_{\mathrm{y},\omega_B} a_{\mathrm{x},\omega_B} a^\dagger_{\mathrm{y},\omega_A} a_{\mathrm{x},\omega_A}:\rangle \\ &= \mathrm{Tr}\{a^\dagger_{\mathrm{y},\omega_B} a_{\mathrm{x},\omega_B} \mathcal{T}\{a_{\mathrm{x},\omega_A}\rho_c a^\dagger_{\mathrm{y},\omega_A}\}\} \in \mathbb{C}, \end{aligned} \tag{14}$$

which all depend on t_A and t_B though this notation has been dropped for brevity. We can define the visibility $\mathcal{V}$ from this expression to be the amplitude of the interference fringes divided by the mean (averaged over ϕ) and it is

$$\mathcal{V}(t_A,t_B) = \frac{2|z|}{x+y}. \tag{15}$$

Conceptually, $\mathcal{V}$ is the visibility of fringes generated by post-selecting photon pairs that arrive within the two-time window $(t_A, t_A + dt)(t_B, t_B + dt)$ as ϕ varies. We note that we may compute the visibility directly from $\tilde{\rho}$ by making the definition $\tilde{x} \equiv \mathrm{Tr}\{a^\dagger_{\mathrm{x},\omega_B} a_{\mathrm{x},\omega_B} \mathcal{T}\{a_{\mathrm{x},\omega_A}\tilde{\rho} a^\dagger_{\mathrm{x},\omega_A}\}\}$, with similar definitions for $\tilde{y}$ and $\tilde{z}$, so that an equivalent expression for the visibility is

$$\mathcal{V}(t_A,t_B) = \frac{2|\tilde{z}|}{\tilde{x}+\tilde{y}}. \tag{16}$$

C. Probability density

We may also compute the joint probability density $\mathcal{P}$ for detecting a photon pair within the two-time window $(t_A, t_A + dt)(t_B, t_B + dt)$, as given in Ref. 17 [Sec. 11.3.7 (d)],

$$\begin{aligned} \mathcal{P}(t_A,t_B) &= \left(\sum_{i,j} \langle :\hat{n}'_{i,\omega_B}(t_B)\hat{n}'_{j,\omega_A}(t_A):\rangle_c \right) \\ &\quad \times \left(1 - \int_0^{t_A} d\tau \sum_j \mathcal{J}'_j \mathcal{T}(\tau,0)\rho(0) \right) \\ &= \sum_{i,j} \langle :\hat{n}'_{i,\omega_B}(t_B)\hat{n}'_{j,\omega_A}(t_A):\rangle_c \mathrm{Tr}\{\tilde{\rho}(t_A)\} \\ &= \kappa^2 \sum_{i,j} \mathrm{Tr}\{\mathcal{J}'_{i,\omega_B}(t_B)\mathcal{T}(t_B,t_A)\{\mathcal{J}'_{j,\omega_A}(t_A)\tilde{\rho}(t_A)\}\} \\ &= \kappa^2(\tilde{x}+\tilde{y}), \end{aligned} \tag{17}$$

where we have again assumed $t_A < t_B$, although similar expressions may easily be derived for $t_A > t_B$. The first factor in the first equality is just the conditional probability density for either the detector to register at times t_A and t_B given no emission beforehand, and the second factor is the probability of emitting zero photons in the interval $[0,t_A]$. The second equality follows from Eq. (10) and its following equations. The third equality follows from Eq. (12) and recalling the fact that $\rho_c(t) = \tilde{\rho}(t)/\mathrm{Tr}\{\tilde{\rho}(t)\}$. Finally, Eq. (17) shows that the probability density does not depend on ϕ—detecting a

photon pair after the interferometer occurs with the same probability density as detecting a photon pair before the interferometer, as expected.

We also define the quantity

$$P=\int_0^\infty\int_0^\infty \mathcal{P}(t_A,t_B)dt_A dt_B. \tag{18}$$

In the presence of spontaneous emission into noncavity photon modes, $P<1$, indicating that not all biexciton decay events will be detected by the photodetectors following the interferometer. We, therefore, interpret P as the reduction factor of the two-photon detection rate, as compared with the biexciton pumping rate.

D. Mean visibility

We now define the mean visibility, which is a figure of merit for the degree of entanglement between the photon pair,

$$\begin{aligned}\overline{\mathcal{V}}&=\frac{1}{P}\int_0^\infty\int_0^\infty \mathcal{V}(t_A,t_B)\mathcal{P}(t_A,t_B)dt_A dt_B\\&=\frac{2\kappa^2}{P}\int_0^\infty\int_0^\infty |\tilde{z}(t_A,t_B)|dt_A dt_B,\end{aligned} \tag{19}$$

where we have divided by P so as to only count those decay events that are detected through the interferometer. If the visibility is unity (i.e., perfect erasure of which-path information), then $\overline{\mathcal{V}}=1$, since the probability density is normalized by P. On the other hand, if $\mathcal{V}$ is less than unity, so will be $\overline{\mathcal{V}}$, therefore, performing a two-photon interference experiment with all photon pairs produced will result in fringes of visibility $\overline{\mathcal{V}}<1$.

We see from Eqs. (16), (17), and (19) that the quantities we are interested in may all be determined directly from $\tilde{\rho}$, which makes calculations we perform in following sections simpler.

E. Phase accumulation

Whilst the visibility is a very important measure of the success of the scheme, since the initial state of the system, $|X\mathrm{x}\rangle|00\rangle|00\rangle$, is not an energy eigenstate, during the emission process, phase will accumulate at different rates on the xx and yy decay paths. The phase difference accumulated between each decay path depends on the emission times of the two photons and is given by $\varphi\equiv\arg\{z(t_A,t_B)\}=\arg\{\tilde{z}(t_A,t_B)\}$, corresponding to emission of a state of the form $|\mathrm{xx}\rangle+e^{i\varphi(t_A,t_B)}|\mathrm{yy}\rangle$. Since, for a given apparatus, φ depends only on the emission times t_A and t_B, this may be calibrated or computed, and hence accounted for, before an interference experiment (or whatever else is intended for the output photon pair) is done. If this phase is ignored, then the mean visibility will be lower than $\overline{\mathcal{V}}$, since the description of the phase-averaged state will be mixed.

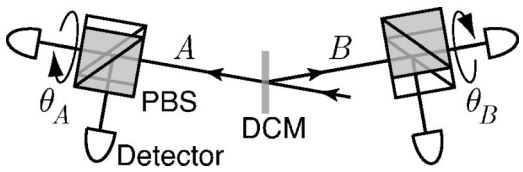

FIG. 4. Schematic setup for performing a CHSH Bell-inequality measurement. Photons of frequency ω_A and ω_B are split with a dichroic mirror and then they travel along paths A and B, respectively, and are measured by rotated polarization-sensitive detectors.

F. Relation to Bell-inequality violations

Instead of passing the photon pair through an interferometer, we could imagine using an ensemble of such states to measure Bell-inequality violations. In particular, we consider violations of a Clauser-Horne-Shimony-Holt (CHSH) inequality, where each photon is measured in one of two nonorthogonal bases specified by the angles θ_A and θ_A' for the photon at frequency ω_A and θ_B and θ_B' for the photon at frequency ω_B,[21] as depicted in Fig. 4.

In terms of mode operators, the CHSH inequality requires the knowledge of correlation functions of the form

$$E(\theta_A,\theta_B)=\frac{\langle:(d_+^\dagger d_+-d_-^\dagger d_-)(c_+^\dagger c_+-c_-^\dagger c_-):\rangle}{\langle:(d_+^\dagger d_++d_-^\dagger d_-)(c_+^\dagger c_++c_-^\dagger c_-):\rangle}, \tag{20}$$

where photon mode annihilation operators c and d are defined as

$$\begin{aligned}c_+&=\sin(\theta_A)a_{\mathrm{y},\omega_A}+\cos(\theta_A)a_{\mathrm{x},\omega_A},\\c_-&=\cos(\theta_A)a_{\mathrm{y},\omega_A}-\sin(\theta_A)a_{\mathrm{x},\omega_A},\\d_+&=\sin(\theta_B)a_{\mathrm{y},\omega_B}+\cos(\theta_B)a_{\mathrm{x},\omega_B},\\d_-&=\cos(\theta_B)a_{\mathrm{y},\omega_B}-\sin(\theta_B)a_{\mathrm{x},\omega_B}.\end{aligned}$$

We have not explicitly included time in these expressions, but we note that operators a_{i,ω_A} act at time t_A and a_{i,ω_B} at t_B. It is straightforward to show that

$$\begin{aligned}c_+^\dagger c_++c_-^\dagger c_-&=a_{\mathrm{y},\omega_A}^\dagger a_{\mathrm{y},\omega_A}+a_{\mathrm{x},\omega_A}^\dagger a_{\mathrm{x},\omega_A},\\c_+^\dagger c_+-c_-^\dagger c_-&=\cos(2\theta_A)(a_{\mathrm{y},\omega_A}^\dagger a_{\mathrm{y},\omega_A}+a_{\mathrm{x},\omega_A}^\dagger a_{\mathrm{x},\omega_A})\\&\quad+\sin(2\theta_A)(a_{\mathrm{y},\omega_A}^\dagger a_{\mathrm{x},\omega_A}+a_{\mathrm{x},\omega_A}^\dagger a_{\mathrm{y},\omega_A}),\end{aligned}$$

with similar results for $d_\pm$. As mentioned earlier, many cross terms in the numerator and denominator of Eq. (20) cancel for the physical situation we consider, e.g., $\langle:a_{\mathrm{x},\omega_A}^\dagger a_{\mathrm{x},\omega_A}a_{\mathrm{y},\omega_B}^\dagger a_{\mathrm{y},\omega_B}:\rangle=0$, so we can write it as

$$\begin{aligned}E(\theta_A,\theta_B)&=\cos(2\theta_A)\cos(2\theta_B)+\frac{z+z^*}{x+y}\sin(2\theta_A)\sin(2\theta_B)\\&=\cos(2\theta_A)\cos(2\theta_B)\\&\quad+\mathcal{V}\cos(\varphi)\sin(2\theta_A)\sin(2\theta_B),\end{aligned} \tag{21}$$

where x, y, and z are defined in Eq. (14).

We now define the quantity

$$\mathcal{B} \equiv E(\theta_A,\theta_B) - E(\theta_A,\theta_B') + E(\theta_A',\theta_B') + E(\theta_A',\theta_B), \tag{22}$$

which, for classically correlated states satisfies $\mathcal{B} \leqslant 2$.[21] This inequality is violated by certain entangled states such as Bell states, which are emitted from the biexciton system. We note that $\mathcal{B}$ depends on t_A and t_B, since $\mathcal{V}$ and φ do, but we leave out the explicit notation. From Eqs. (21) and (22), we derive a linear relationship between $\mathcal{B}$ and $\mathcal{V}$ given by

$$\begin{aligned}\mathcal{B} = &\cos(2\theta_A)[\cos(2\theta_B) - \cos(2\theta_B')] \\ &+ \cos(2\theta_A')[\cos(2\theta_B) + \cos(2\theta_B')] \\ &+ \mathcal{V}\cos(\varphi)\{\sin(2\theta_A)[\sin(2\theta_B) - \sin(2\theta_B')] \\ &+ \sin(2\theta_A')[\sin(2\theta_B) + \sin(2\theta_B')]\}. \end{aligned} \tag{23}$$

We consider a special choice of angles that maximally violate the CHSH inequality, $\theta_A = 0, \theta_B = \vartheta, \theta_A' = 2\vartheta$, and $\theta_B' = 3\vartheta$, and using Eq. (21) in the expression for $\mathcal{B}$, we find that

$$\begin{aligned}\mathcal{B} = &\cos(2\vartheta)[3 - 2\cos(4\vartheta) + \cos(8\vartheta)] \\ &+ 8\cos(2\vartheta)^3 \sin(2\vartheta)^2 \mathcal{V}\cos(\varphi). \end{aligned} \tag{24}$$

For $\mathcal{V} = 1$, this gives $\mathcal{B} = 3\cos(2\vartheta) - \cos(6\vartheta)$, which has a maximum at $\vartheta = \pi/8$ of $2\sqrt{2} > 2$, violating the CHSH inequality. At $\vartheta = \pi/8$, Eq. (24) reduces to

$$\mathcal{B} = \sqrt{2}[1 + \mathcal{V}\cos(\varphi)], \tag{25}$$

which is plotted in Fig. 5 (lower curve). We also show the maximum value of $\mathcal{B}$ for each value of $\mathcal{V}$ (upper curve), allowing ϑ to vary. The upper curve crosses $\mathcal{B} = 2$ at $\mathcal{V}\cos(\varphi) \approx 0.316$, whilst the lower curve crosses at $\mathcal{V}\cos(\varphi) = \sqrt{2} - 1 \approx 0.414$.

From these results, we see that $\mathcal{V}$ and $\mathcal{B}$ are very closely related quantities. Since $\mathcal{B}$ may be computed from $\mathcal{V}$ for arbitrary angles, we will base our computations on $\mathcal{V}$, from which a reasonable estimate for the maximum value $\mathcal{B}$ may be evaluated using Eq. (25). Finally, we define the quantity $\overline{\mathcal{B}}$ as

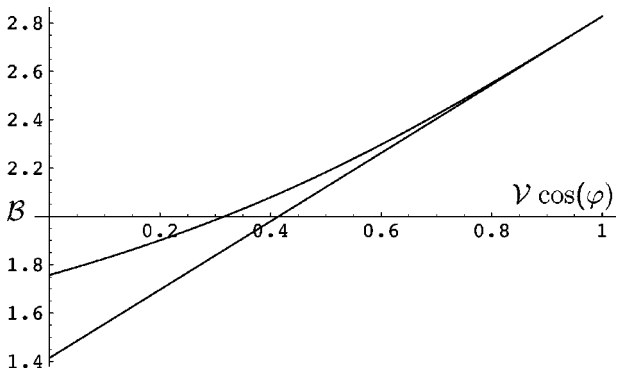

FIG. 5. The quantity $\mathcal{B}$ versus $\mathcal{V}$. The lower curve is $\mathcal{B}$ for $\vartheta = \pi/8$. The upper curve is the maximum value of $\mathcal{B}$ for the corresponding value of $\mathcal{V}$, allowing ϑ to change with $\mathcal{V}$.

$$\overline{\mathcal{B}} = \frac{1}{P}\int_0^\infty \int_0^\infty \mathcal{B}(t_A,t_B)\mathcal{P}(t_A,t_B)\,dt_A dt_B, \tag{26}$$

where we have again divided by P in order to count only those photon pairs that are detected in the experiment.

G. Phase-averaged Bell-inequality violation

Comparing $\overline{\mathcal{B}}$ with Eq. (24) or Eq. (25), we see that we need to compute the quantity

$$\frac{1}{P}\int_0^\infty \int_0^\infty \mathcal{P}\mathcal{V}\cos(\varphi)\,dt_A dt_B.$$

We generalize this to account for the possibility of adding a fixed relative phase ϕ to one decay path (e.g., by adding a phase plate on the *y*-polarized photon path, as in the interferometer stage of Fig. 3), so that $\cos(\varphi) \to \cos(\varphi + \phi)$. We maximize the above integral over ϕ to arrive at the *phase-averaged visibility*

$$\mathcal{Q} = \frac{1}{P}\sqrt{\left(\int_0^\infty \int_0^\infty \mathcal{P}\mathcal{V}\cos(\varphi)\,dt_A dt_B\right)^2 + \left(\int_0^\infty \int_0^\infty \mathcal{P}\mathcal{V}\sin(\varphi)\,dt_A dt_B\right)^2}. \tag{27}$$

The phase-averaged visibility $\mathcal{Q}$ gives the visibility of the fringes in a two-photon interference experiment, where no attempt is made to resolve the phase accumulation. In regard to a CHSH-inequality violation experiment without sufficiently fast time-resolved detection, violations may still be seen if $\mathcal{Q} > 0.316$, since the functional relationship between $\mathcal{Q}$ and $\overline{\mathcal{B}}$ is the same as that between $\mathcal{B}$ and $\mathcal{V}\cos(\varphi)$, as shown in Fig. 5.

V. ANALYTICAL RESULT FOR BALANCED CAVITY

We now show that for a balanced cavity (i.e., $\delta_A = \delta_B = \Delta/2$, $q_1 = q_3$, and $q_2 = q_4$), in the absence of spontaneous emission and dephasing, $\Gamma_d = \Gamma_s = 0$, the model predicts that the visibility is unity for all (t_A, t_B). Since we assume $\Gamma_d = \Gamma_s = 0$, we may write the unnormalized density matrix as $\tilde{\rho}(t) = |\tilde{\psi}(t)\rangle\langle\tilde{\psi}(t)|$ and then Eq. (9) may be written as a Schrödinger equation

$$\frac{d}{dt}|\tilde{\psi}(t)\rangle = -i\mathcal{H}|\tilde{\psi}(t)\rangle \tag{28}$$

for the state vector, $|\tilde{\psi}(t)\rangle$, with a non-Hermitian effective Hamiltonian given by

$$\mathcal{H} = H - i\kappa/2(\hat{n}_{\mathsf{x},\omega_A} + \hat{n}_{\mathsf{y},\omega_A} + \hat{n}_{\mathsf{x},\omega_B} + \hat{n}_{\mathsf{y},\omega_B}). \tag{29}$$

We write the solution to Eq. (28) as $|\tilde{\psi}(t)\rangle = e^{-i\mathcal{H}t}|\tilde{\psi}(0)\rangle$. The smooth evolution is of course punctuated by quantum jumps, corresponding to photon detections following the interferometer.

Reformulating the equations of motion in terms of quantum trajectories[17] has several advantages, and most obviously it reduces the number of unknown quantities, since we can now solve for the state vector rather than the density matrix. It is straightforward to show that the effective Hamiltonian $\mathcal{H}$ only couples states within the same excitation-number subspace. Coupling between the zero-, one-, and two-excitation subspaces (denoted $\mathcal{S}_0, \mathcal{S}_1$, and $\mathcal{S}_2$ respectively) occurs only during the jumps, and the excitation number irreversibly decreases by one at each jump as photons leave the cavity. Thus, for the smooth evolution between jumps, we may consider the evolution restricted to states within each $\mathcal{S}_j$ independently, and for each $\mathcal{S}_j$ we consider the effective Hamiltonian $\mathcal{H}_j$ restricted to that subspace and acting on the state vector $|\tilde{\psi}(t)\rangle_j$.

Using the quantum trajectories formalism, we find

$$\tilde{x} = \langle\tilde{\psi}_{\mathsf{x}}(t_A,t_B)|\tilde{\psi}_{\mathsf{x}}(t_A,t_B)\rangle, \tag{30a}$$

$$\tilde{y} = \langle\tilde{\psi}_{\mathsf{y}}(t_A,t_B)|\tilde{\psi}_{\mathsf{y}}(t_A,t_B)\rangle, \tag{30b}$$

$$\tilde{z} = \langle\tilde{\psi}_{\mathsf{y}}(t_A,t_B)|\tilde{\psi}_{\mathsf{x}}(t_A,t_B)\rangle, \tag{30c}$$

where, assuming $t_A < t_B = t_A + \tau$, we have defined

$$\begin{aligned}|\tilde{\psi}_i(t_A,t_B)\rangle &= a_{i,\omega_B}e^{-i\mathcal{H}_1\tau}a_{i,\omega_A}|\tilde{\psi}(t_A)\rangle \\ &= a_{i,\omega_B}e^{-i\mathcal{H}_1\tau}a_{i,\omega_A}e^{-i\mathcal{H}_2 t_A}|\tilde{\psi}(0)\rangle.\end{aligned} \tag{31}$$

A very similar expression exists for $t_A > t_B$, and the following reasoning applies equally to both cases. The state vector $|\tilde{\psi}_i(t_A,t_B)\rangle \in \mathcal{S}_0$, since the initial condition $|\psi(0)\rangle = |XX\rangle|00\rangle|00\rangle \in \mathcal{S}_2$ and the effect of the two annihilation operators in Eq. (31) is to reduce the excitation number by 2.

The one-dimensional subspace $\mathcal{S}_0$ is spanned by the system ground state $|\mathsf{G}\rangle|00\rangle|00\rangle$, so a state $|\tilde{\psi}(t)\rangle \in \mathcal{S}_0$ is mapped smoothly to a scalar $\tilde{\psi}(t)$ by the trivial mapping $\tilde{\psi}(t) \equiv (\langle\mathsf{G}|\langle 00|\langle 00|)|\tilde{\psi}(t)\rangle$. We may, therefore, write $\tilde{x}, \tilde{y}$ and $\tilde{z}$ in terms of the scalar quantities $\tilde{\psi}_{\mathsf{x}}(t_A,t_B)$ and $\tilde{\psi}_{\mathsf{y}}(t_A,t_B)$: $\tilde{x} = \tilde{\psi}_{\mathsf{x}}^*\tilde{\psi}_{\mathsf{x}}, \tilde{y} = \tilde{\psi}_{\mathsf{y}}^*\tilde{\psi}_{\mathsf{y}}$ and $\tilde{z} = \tilde{\psi}_{\mathsf{y}}^*\tilde{\psi}_{\mathsf{x}}$, where we have dropped the time-dependent notation for clarity.

In what follows, we establish that for a balanced cavity, $\tilde{\psi}_{\mathsf{x}}$ and $\tilde{\psi}_{\mathsf{y}}$ are related by a unitary factor. This means that they have the same amplitude, from which it follows that the visibility is unity for a balanced cavity. We do this by considering the transformation of the effective Hamiltonian and state vector under exchange of the polarization, $|X\mathsf{x}\rangle \leftrightarrow |X\mathsf{y}\rangle$ and $|01\rangle \leftrightarrow |10\rangle$. This transformation, denoted hereafter by $^{\#}$, is just a permutation on the basis elements, leaving the two elements $|XX\rangle|00\rangle|00\rangle$ and $|\mathsf{G}\rangle|00\rangle|00\rangle$ invariant. A matrix representation of $^{\#}$ shows that it is both orthogonal and symmetric.

Consider evolution in $\mathcal{S}_2$. Swapping x and y polarizations maps $\mathcal{H}_2 \to \mathcal{H}_2^{\#} = -\mathcal{H}_2^*$ and $|\tilde{\psi}(t)\rangle_2 \to |\tilde{\psi}(t)\rangle_2^{\#}$. As a result the time evolution operator $(e^{-i\mathcal{H}_2 t})^{\#} = e^{-i\mathcal{H}_2^{\#}t} = e^{i\mathcal{H}_2^* t}$ when acting on states in $\mathcal{S}_2$. We note in passing that for an unbalanced cavity or coupling $\mathcal{H}_2^{\#} \neq -\mathcal{H}_2^*$, which is why it is critical that the cavity be balanced for this argument to be valid.

A similar result applies to evolution in $\mathcal{S}_1$, except that the effective Hamiltonian $\mathcal{H}_1$ does not transform under polarization swapping quite as simply. Instead, it may be shown that $\mathcal{H}_1 - H_d \to \mathcal{H}_1^{\#} - H_d^{\#} = -(\mathcal{H}_1^* - H_d)$, where H_d is a Hermitian matrix acting on elements of $\mathcal{S}_1$ and satisfies $[\mathcal{H}_1, H_d] = 0$. Thus, $\mathcal{H}_1^{\#} = -\mathcal{H}_1^* + H_d + H_d^{\#}$ and $(e^{-i\mathcal{H}_1 t})^{\#} = e^{-i\mathcal{H}_1^{\#}t} = e^{i\mathcal{H}_1^* t}e^{-i(H_d + H_d^{\#})t}$. The factor $U_d(t) = e^{-i(H_d + H_d^{\#})t}$ is unitary, since H_d is Hermitian. In particular, $U_d(t)$ acts on states of the form $a_{i,\omega_A}e^{-i\mathcal{H}t_A}|\tilde{\psi}(0)\rangle \in \mathcal{S}_1$ in a simple way: it multiples the state by a time-dependent unitary scalar, $e^{i\theta t}$.

Having established the effect of $^{\#}$ on the time evolution operator acting on $\mathcal{S}_1$ and $\mathcal{S}_2$ we see that, for example,

$$\begin{aligned}|\tilde{\psi}_{\mathsf{x}}(t_A,t_B)\rangle^{\#} &= [a_{\mathsf{x},\omega_B}e^{-i\mathcal{H}_1\tau}a_{\mathsf{x},\omega_A}e^{-i\mathcal{H}_2 t_A}|\tilde{\psi}(0)\rangle]^{\#} \\ &= a_{\mathsf{y},\omega_B}e^{-i\mathcal{H}_1^{\#}\tau}a_{\mathsf{y},\omega_A}e^{-i\mathcal{H}_2^{\#}t_A}|\tilde{\psi}(0)\rangle, \\ &= e^{i\theta\tau}a_{\mathsf{y},\omega_B}e^{i\mathcal{H}_1^*\tau}a_{\mathsf{y},\omega_A}e^{i\mathcal{H}_2^* t_A}|\tilde{\psi}(0)\rangle, \\ &= e^{i\theta\tau}(a_{\mathsf{y},\omega_B}e^{-i\mathcal{H}_1\tau}a_{\mathsf{y},\omega_A}e^{-i\mathcal{H}_2 t_A}|\tilde{\psi}(0)\rangle)^*, \\ &= e^{i\theta\tau}|\tilde{\psi}_{\mathsf{y}}(t_A,t_B)\rangle^*.\end{aligned} \tag{32}$$

The second line follows since $|\tilde{\psi}(0)\rangle^{\#} = |XX\rangle|00\rangle|00\rangle^{\#} = |XX\rangle|00\rangle|00\rangle = |\tilde{\psi}(0)\rangle$ and $a_{\mathsf{x}}, \omega^{\#} = a_{\mathsf{y}}, \omega$ and the third line follows by considering the arguments in the preceding two paragraphs.

On the other hand, since $|\tilde{\psi}_{\mathsf{x}}(t_A,t_B)\rangle \in \mathcal{S}_0$ it is evident that $|\tilde{\psi}_{\mathsf{x}}(t_A,t_B)\rangle^{\#} = |\tilde{\psi}_{\mathsf{x}}(t_A,t_B)\rangle$ as $|\mathsf{G}\rangle|00\rangle|00\rangle$ is invariant under $^{\#}$. Together with Eq. (32), this implies $|\tilde{\psi}_{\mathsf{x}}(t_A,t_B)\rangle = e^{i\theta\tau}|\tilde{\psi}_{\mathsf{y}}(t_A,t_B)\rangle^*$, and we conclude that $\tilde{\psi}_x = e^{i\theta\tau}\tilde{\psi}_y^*$. It follows that $\tilde{x} = \tilde{\psi}_{\mathsf{x}}^*\tilde{\psi}_{\mathsf{x}} = \tilde{\psi}_{\mathsf{y}}^*\tilde{\psi}_{\mathsf{y}} = \tilde{y}$, and also $|\tilde{z}| = |\tilde{\psi}_{\mathsf{y}}^*\tilde{\psi}_{\mathsf{x}}| = |e^{-i\theta\tau}\tilde{\psi}_{\mathsf{x}}^2| = \tilde{x}$. Using these two results and Eq. (16) we see immediately that for a balanced cavity $\mathcal{V} = 1$, proving that the visibility is unity for all times.

VI. NUMERICAL RESULTS

In this section, we present the results of computations for $\overline{\mathcal{V}}$ for unbalanced systems, and results for $\mathcal{Q}$ which characterize the extent to which Bell-inequality violations may be observed. For the problem parameters, we take experimen-

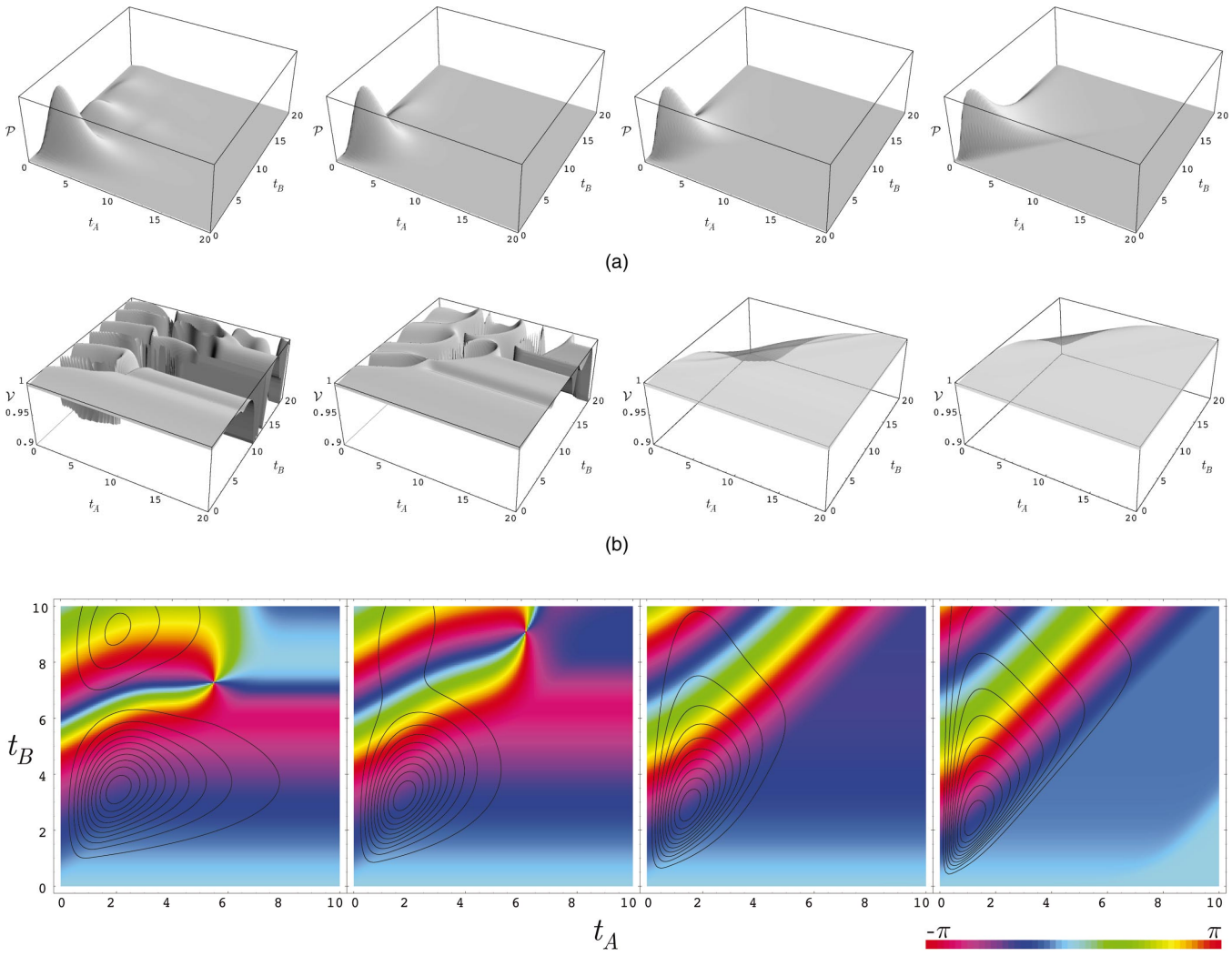

FIG. 6. (Color) In each row, from left to right, κ=0.5,1,2,4 and $\Gamma_d=\Gamma_s=0$ in all figures. (a) Time-dependent probability distribution, $\mathcal{P}(t_A,t_B)$, for a balanced system. (b) Visibility, $\mathcal{V}(t_A,t_B)$, for an unbalanced system, where $q_{1,2,3}=1$ and $q_4=1.1$. (c) (Color) Relative phase, $\varphi(t_A,t_B)$, for a balanced system. Superimposed on each panel is a contour plot of $\mathcal{P}$.

tally relevant values typical for GaAs self-assembled dots $\Delta=50$ μeV,[22] $\xi=0.5$ meV, $q=50$ μeV,[23,24] and $\kappa>100$ μeV, though values of κ much lower than this may be possible with novel hemispherical cavities.[24] Throughout this section, we rescale all energies so that $q_i=1$, $\Delta=1$, $\xi=10$. Time is also rescaled accordingly, so one time unit corresponds to 83 ps. Figure 6(a) shows plots of the probability distribution of emission times for a balanced cavity with no leakage channels. Numerically computed visibility is unity to within numerical accuracy and $\overline{\mathcal{V}}=1$ to within 10^{-4}, when integrating out to $t_A=t_B=200$. Notice Rabi oscillations in emission time for strong coupling ($\kappa<q_i=1$) and exponential decay for weak coupling ($\kappa>q$). For strong coupling, there is a significant probability of emitting photons in either order, but in weak coupling, the order $t_B>t_A$ is strongly favored indicated by the sharp edge along $t_A=t_B$.

We also note that in the weak coupling regime, $\mathcal{P}$ has a tendency to broaden with increasing κ, which is somewhat counterintuitive, since larger κ corresponds to a more leaky cavity, and one would expect the photon component of the internal state to leak away more rapidly. However, this phenomenon may also be seen in the much simpler case of a single two-level atom interacting with coupling rate q with a single optical mode of a leaky cavity. In that case it is straightforward to show that there is in eigenvalue of the effective Hamiltonian for the open system given by $q^2\kappa^{-1}/2+O(\kappa^{-2})$, which corresponds to a long-time constant for large κ. When $\kappa\approx q$, there is a kind of impedance matching, and the temporal extent of $\mathcal{P}$ is smallest.

As established previously, the visibility is unity for a balanced system. For an unbalanced system, the visibility drops below unity, as shown in Fig. 6(b) where $q_4=1.1$ (with $q_{1,2,3}=1$), for different values of κ. The probability density $\mathcal{P}$ for this case looks very similar to Fig. 6(a) so is not shown here. We note that the visibility depends only on t_B when $t_A>t_B$, i.e., it is frozen at the value it reaches at t_B. Notice that the probability $\mathcal{P}$ of emitting a photon pair is small at the same time that $\mathcal{V}$ has large excursions from unity, which means $\overline{\mathcal{V}}$ is not affected as much as one might expect, given the large fluctuations in $\mathcal{V}$. The difference between strong

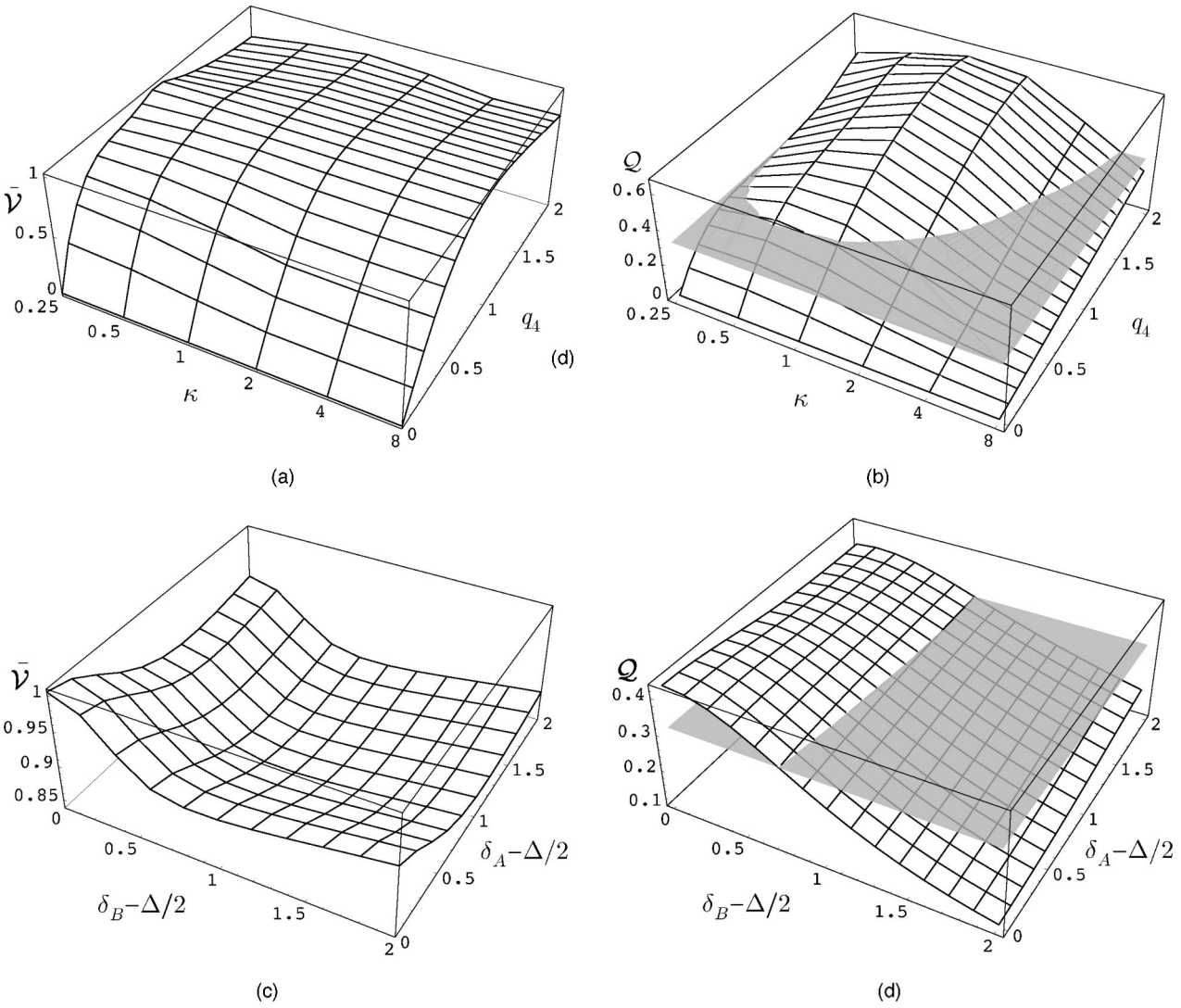

FIG. 7. Dependence of (a) $\overline{\mathcal{V}}$ and (b) $\mathcal{Q}$ on q_4 for various κ. Dependence of (c) $\overline{\mathcal{V}}$ and (d) $\mathcal{Q}$ on δ_A and δ_B. $\overline{\mathcal{V}}$ and $\mathcal{Q}$ are not sensitive to the sign of δ_A or δ_B so other quadrants look similar and are not displayed. The gray plane at $\mathcal{Q}=0.316$ demarks the threshold, above which Bell-inequality violations may be observed.

and weak couplings is striking, again with oscillations being replaced by decay.

The relative phase φ is shown in Fig. 6(c) for a balanced system. Also superimposed on each panel is a contour plot of the emission probability density $\mathcal{P}$. In the strong-coupling regime, during Rabi oscillation peaks, the phase accumulates relatively slowly, with rapid phase rotations in between. In the weak-coupling regime, the phase accumulates at a fairly constant rate, which is roughly proportional to Δ. The diagonal stripes indicate that in weakly coupled cavities, the phase accumulation depends only on the time interval between photon emission, t_B-t_A, in contrast to the much more complicated dependence of the phase in the strong-coupling regime, which shows phase singularities.

Figure 7(a) shows the variation of $\overline{\mathcal{V}}$ versus q_4 for various κ. For $q_4=0$, one decay path is turned off so we expect completely nonentangled photon pairs, and this is evident in Fig. 7(a) as $\overline{\mathcal{V}}=0$ when $q_4=0$. We also expect that $\overline{\mathcal{V}}=1$ when $q_4=1$, since then the couplings are again balanced, and this also is evident in Fig. 7(a). The variation with q_2 is identical to that displayed here, whilst the variation of $\overline{\mathcal{V}}$ with q_1 and q_3 is qualitatively very similar, so it is not shown here.

As discussed earlier, $\mathcal{Q}$ is a significant quantity that determines whether the photon pair can produce Bell-inequality violations in the absence of time-resolved detection, so that the phase is ignored. In particular, as shown in Fig. 5, whenever $\mathcal{Q}>0.316$, then the photon pair can produce Bell-inequality violations, even in the case that φ is ignored. Figure 7(b) shows $\mathcal{Q}$ for the same values of q_4 and κ as in Fig. 7(a), where the gray plane demarks the threshold, $\mathcal{Q}=0.316$, to see Bell-inequality violation, as it will in all following plots of $\mathcal{Q}$. Whilst $\mathcal{Q}$ is everywhere less than unity, there are parameter values where Bell-inequality violation may still be observed without using time-resolved detection.

If the cavity geometry is such that $\delta_A\neq\Delta/2$ or $\delta_B\neq\Delta/2$,

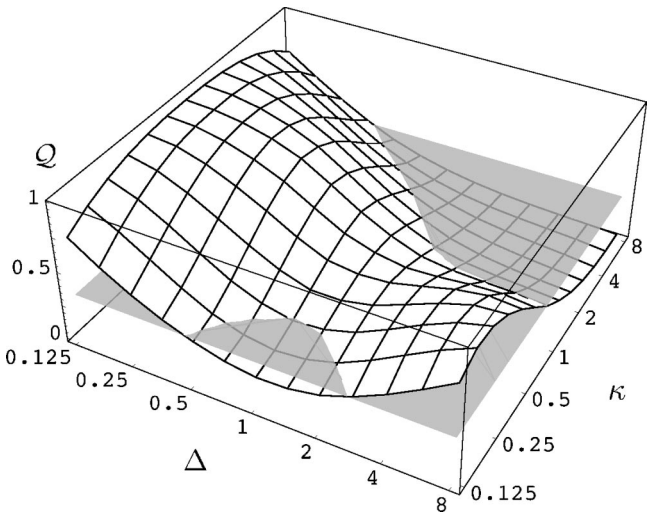

FIG. 8. $\mathcal{Q}$ versus Δ for κ. Varying Δ changes the rate of phase accumulation between the photon detection events. Gray plane as in Fig. 7.

then the cavity is unbalanced. This has the effect of reducing $\overline{\mathcal{V}}$ below unity, as shown in Fig. 7(c). Results are only displayed for $\delta_{A,B}>\Delta/2$, but the other quadrants are similar. Figure 7(d) shows $\mathcal{Q}$ for the same parameter values, again with the plane denoting the threshold for Bell-inequality violation.

The phase accumulates in between the photon detection events roughly at a rate proportional to Δ, the splitting due to dot asymmetry, and this directly affects $\mathcal{Q}$, since for smaller Δ, we expect the phase to be more nearly constant over the photon emission lifetime. This may be seen in Fig. 8, where for small Δ, $\mathcal{Q}$ approaches unity, although Bell-inequality violation may still be seen for a wide range of κ and Δ.

The two different leakage channels that we consider in this paper are spontaneous emission into noncavity modes, which occurs at a rate Γ_s, and dephasing which happens at a rate Γ_d.

The spontaneous emission does not affect the visibility of those photon pairs that arrive at the detector, but it does change the rate of detection, since some photons are lost. The reduction in photon detection rate, given by P, is shown in Fig. 9(a). The roll-off in P is roughly proportional to Γ_s^{-1}. Surprisingly, the spontaneous emission enhances $\mathcal{Q}$, which may be seen in Fig. 9(b), although, we note that the source is then no longer deterministic. Experimentally, the fraction of photons emitted into the cavity mode, known as the β factor, has been observed as high as 0.83 (Ref. 25) and there is a suggestion that $\beta=0.9$ may be attainable.[26] Interpreting P as the β factor, from Fig. 9(a), we surmise that for $P\approx 0.9$, the experimentally relevant range of the spontaneous emission rate is $\Gamma_s \ll 0.1=5\ \mu$eV, which is a regime in which spontaneous emission is negligible.

Figures 9 and 9(d) show the effect of the phenomenological dephasing term Γ_d for different values of κ. $\overline{\mathcal{V}}$ and $\mathcal{Q}$ decay roughly as Γ_d^{-1}. In all panels of Fig. 9, there is a peak along $\kappa\approx q$, which is due to the fact that $\mathcal{P}$ is temporally the narrowest when this condition is met, and hence there is less time for leakage to take place. For very low temperatures, around 1 K or lower, pure dephasing rates have been observed to be around 1 μeV,[27] corresponding to $\Gamma_d=0.02$, which is negligible. For higher temperatures, the pure dephasing has been observed to increase at roughly 0.5–1.6 μeV/K.[27,28] From Fig. 7(d), the pure dephasing becomes important near $\Gamma_d \lesssim 1$, corresponding to a temperature between 30 and 100 K for the experimentally relevant range given above.

VII. DISCUSSION

In the preceding section, we found that the numerical results for a balanced system concur with the analytical result derived in Sec. V, where we established that the visibility is unity in this case. We also noted that $\overline{\mathcal{V}}$ is degraded by any effect which may cause the cavity or couplings to be unbalanced. Imperfections in the cavity geometry will result in an unbalanced cavity so $\delta_{A,B}\neq\Delta/2$, and it was shown above that this reduces $\overline{\mathcal{V}}$. Similarly, unbalanced coupling constants also results in decreased visibility.

Both of these effects may be understood heuristically using a much simpler model which captures the gross features seen in Figs. 6(b) and 7(c). First, we note that a two-photon state given by $\alpha_{\mathsf{x}}|\mathsf{xx}\rangle+\alpha_y|\mathsf{yy}\rangle$ will produce two-photon interference fringes with visibility

$$V=\frac{2|\alpha_{\mathsf{x}}\alpha_{\mathsf{y}}|}{|\alpha_{\mathsf{x}}|^2+|\alpha_{\mathsf{y}}|^2}. \tag{33}$$

Second, we make two *ad hoc* simplifications of the level structure of the quantum dot shown in Fig. 1(a). These simplifications are (i) to ignore the crystal ground state $|\mathsf{G}\rangle$ and the corresponding transitions thereto, and (ii) to treat the remaining three-level system, composed of $|XX\rangle$, $|X\mathsf{x}\rangle$, and $|X\mathsf{y}\rangle$ as a pair of independent two-level systems (TLS), $\{|g\rangle_1,|e\rangle_1\}$, and $\{|g\rangle_2,|e\rangle_2\}$, each of which interact with one of a pair of degenerate cavity modes distinguished by polarization. With these two assumptions, the energy-level structure becomes that shown in Fig. 10(a).

The physical motivation for these seemingly arbitrary assumptions is first that once the biexciton decay proceeds along the x- or y-polarized paths of Fig. 1(a), the resulting two-photon amplitudes $\alpha_{\mathsf{x,y}}$ are determined, even though the dynamics of the emission are not complete. Thus, the two-photon amplitudes are largely determined by the initial single-photon decay process, justifying (i). Second, while the sum of probabilities to take the x- or y-polarization decay paths is unity, apart from this constraint the rate equations for the two decay processes are otherwise uncoupled, so that the system is similar to a pair of uncoupled TLS's, one for each decay path, justifying (ii). Ultimately, this highly simplified model will be verified by its qualitative agreement with the more realistic model discussed throughout this paper, and its value is in the intuition it lends about the origin of the effects seen in the numerical calculations.

A TLS interacting with a cavity mode is well understood in terms of the Jaynes-Cummings model.[14] For TLS's ini-

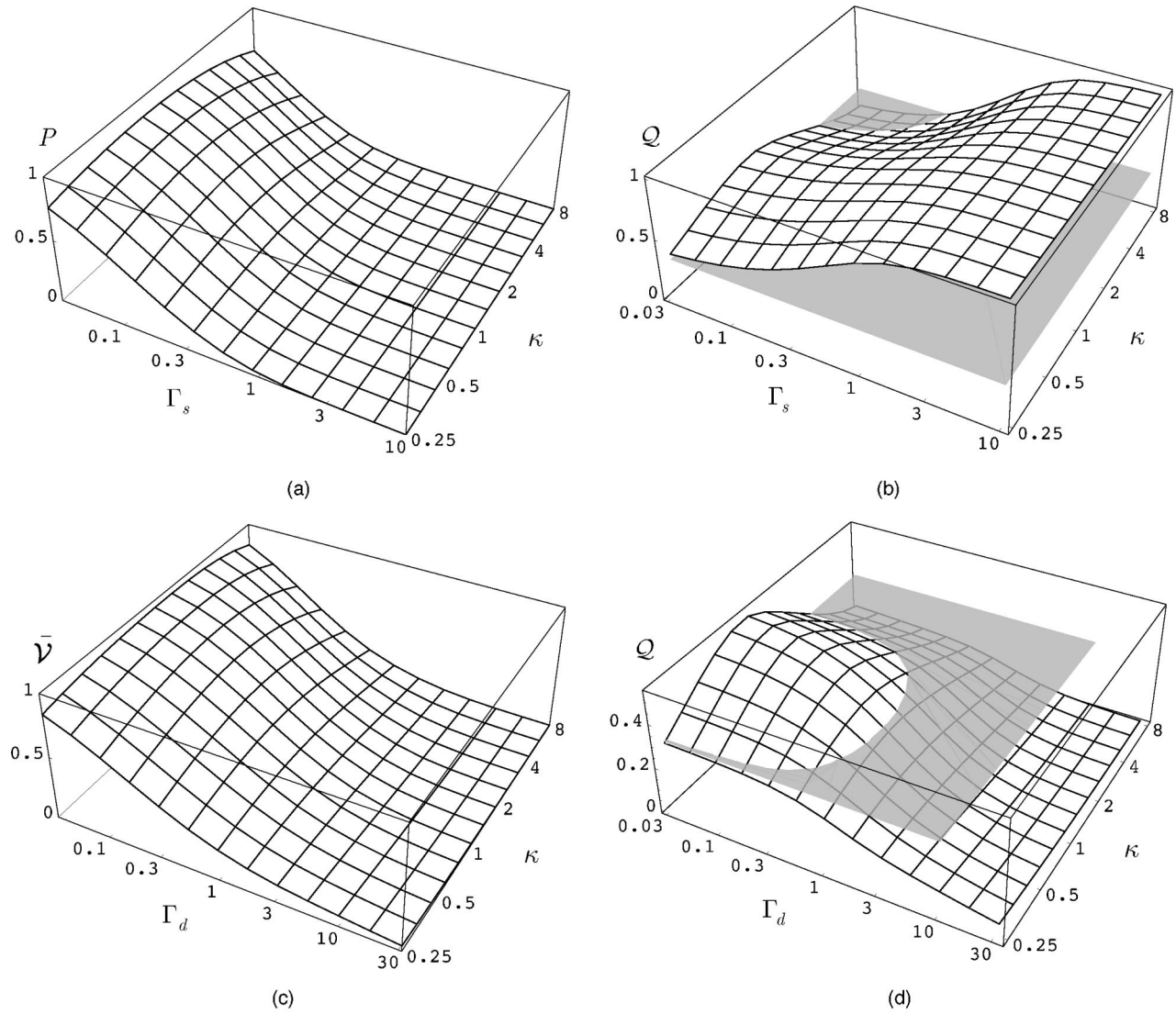

FIG. 9. (a) P and (b) $\mathcal{Q}$ versus spontaneous emission Γ_s, for different values of κ. (c) $\bar{\mathcal{V}}$ and (d) $\mathcal{Q}$ versus dephasing rate Γ_d for various κ. Gray plane as in Fig. 7.

tially in the state $|e\rangle_i$ ($i=1,2$ is the TLS label) with energy spacings ν_i, oscillator frequency ω_i, and detuning $\delta_i=\nu_i-\omega_i$, with TLS-cavity coupling rate Ω_i [see Fig. 10(a)], the time-averaged photon population is given by $p_i=\Omega_i^2/(2R_i^2)$, where $R_i=\sqrt{\delta_i^2+\Omega_i^2}$, and we conclude that the average amplitude of photon occupation satisfies

$$|\alpha_{x,y}|=\frac{\Omega_{1,2}}{\sqrt{2}R_{1,2}}. \tag{34}$$

We now compare the predictions of this simple model with the more complete one for an unbalanced cavity, wherein the cavity mode is not tuned to the mean of the transition frequencies, $\omega\neq(\nu_1+\nu_2)/2$. If the TLS's are detuned by an amount $\delta_{1,2}=\delta\mp D/2$, respectively, from the degenerate cavity modes, [see Fig. 10(a)], each with the same cavity-coupling strength $\Omega_{1,2}=\Omega$, the visibility is then given by

$$V=\frac{2R_1R_2}{R_1^2+R_2^2}, \tag{35}$$

where we have taken $|\alpha_{x,y}|$ from Eq. (34). This expression is plotted in Fig. 10(b) as a function of δ (using $\Omega=0.61$, $D=1$) along with $\bar{\mathcal{V}}$ (using $q_{1,2,3,4}=1$, $\kappa=0.4$, $\Delta=1$, $\delta_A=\Delta/2$, $\xi=10$, $\Gamma_{d,s}=0$). Clearly, the forms of the two traces are in qualitative agreement demonstrating the heuristic validity of the simple model. The value $\Omega=0.61$ is selected to fit Eq. (35) to the numerically computed $\bar{\mathcal{V}}$, but it is of the same order as $q_i=1$.

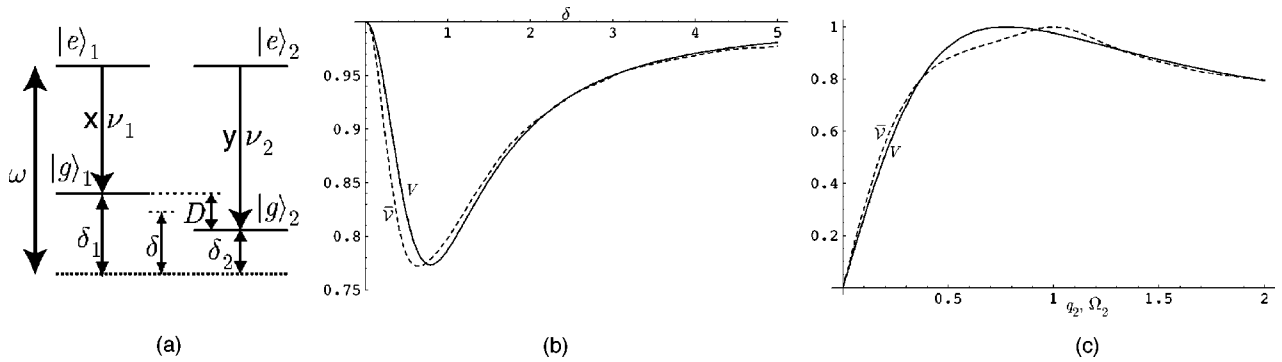

FIG. 10. (a) Energy levels for independent two-level system. (b) Equation (35) (solid) versus δ and also $\bar{\mathcal{V}}$ (dotted) versus δ_B. (c) Equation (36) (solid line) versus δ and also $\bar{\mathcal{V}}$ (dotted line) versus δ_B. Parameters as usual except $\kappa=0.4$.

We also compare the predictions of the simple model for unbalanced coupling to the realistic model, and so we take $\Omega_1 \neq \Omega_2$, but assume the detunings between the two-level systems and their respective harmonic oscillators are equal, $\delta_1 = -\delta_2 = \delta$. It is straightforward to show that

$$V = \frac{2R_1\Omega_1 R_2\Omega_2}{(R_1\Omega_1)^2 + (R_2\Omega_2)^2}, \tag{36}$$

which is plotted in Fig. 10(c) (using $\Omega_1 = 0.42$, $\delta = 1.69$ both fitted parameters), along with $\bar{\mathcal{V}}$ [other parameter values as in Fig. 10(b)].

The simple, heuristic model of two uncoupled two-level systems predicts a visibility V that is qualitatively in agreement with $\bar{\mathcal{V}}$ calculated using the complete model discussed in earlier sections. Thus, we can understand the most significant effect of variation of q_i and δ_i on $\bar{\mathcal{V}}$ is to change the relative amplitudes to take each of the two decay paths illustrated in Fig. 1(a). Since the photon pair is only maximally entangled when the amplitudes of the $|\mathrm{xx}\rangle$ and $|\mathrm{yy}\rangle$ components are equal in magnitude [i.e., for the state $(|\mathrm{xx}\rangle + e^{-i\phi}|\mathrm{yy}\rangle)/\sqrt{2}$], parameter variations that result in unequal decay path amplitudes result in submaximally entangled photon pairs. Such parameter variations correspond directly to the situation of an unbalanced system.

The analysis above gives us some further insight into the decay process. The maximum amplitude of the photon excitation is Ω^2/R^2 and so the leakage rate of photons from the cavity will be suppressed by this factor. That is, we expect that the rate of decay of excitation from the cavity will be roughly $\kappa\Omega^2/(\Omega^2+\delta^2)$. Therefore, as the detuning δ increases, the photon emission rate slows roughly as $\sim 1/\delta^2$ for $\delta > \Omega$. This will mean that for detunings significantly larger than the coupling strength, leakage effects will become significant—the lifetime of the excitation in the cavity will become comparable to the decay rate for dephasing or spontaneous emission.

It is also worth noting that when $\delta \sim 2\xi$ (i.e., the exciton-cavity detuning is near the biexciton shift), the model developed in Sec. II breaks down, since significant cross coupling between exciton states and cavity modes will set in.

Spontaneous emission decreases the detection probability, which could be corrected with post selection, since only events in which two-photons are registered count towards the measurement, and as mentioned previously, experimental work has shown that this is negligible for experimentally relevant systems.[26] Dephasing of intermediate states decreases the visibility exponentially in time. Temperatures of a few Kelvin provide sufficiently low dephasing rates such that it is negligible, but the excitonic dephasing becomes important at temperatures of several tens of Kelvin.[27,28] In principle, these effects may be distinguished using sufficiently fast time-resolved spectroscopy, since spontaneous emission will result in fewer photons reaching the detector, whereas dephasing would result in a time-dependent visibility that degrades exponentially with time.

So far, we have not addressed the issue of how to experimentally construct a cavity with the required spectrum, shown in Fig. 1(a), and a detailed proposal for its implementation is beyond the scope of this paper. The enhanced exciton emission into the cavity mode is known as the Purcell effect and requires small cavity volumes, so that the exciton-cavity mode coupling strength is large and the density of available photon modes is small.[26,29] Thus, small cavities are necessary, and the high Purcell factors have been demonstrated experimentally in single-wavelength sized cavities.[26,30]

In contrast to the need for small cavities is the relatively small biexciton shift, 2ξ, which is around 1 meV. In order for a single Fabry-Perót resonator to accommodate modes spaced by 1 meV (i.e., the free spectral range, FSR), the cavity length would need to be of the order of 100 μm or more. For monolithic dot-in-cavity systems, this is too long for several reasons, primarily because the Purcell factor for such a long (planar) cavity would be small, so leakage to other modes would be large, and also because growth of such a large heterostructure would be prohibitively difficult. As a result, the cavity to which we have been referring throughout this paper would need to be based on a more complicated geometry than merely a pair of planar distributed Bragg reflectors (DBR) forming a linear resonator.

We stress that a more complex geometry is not just a requirement of this proposal, but that it would be necessary for a system even with symmetric quantum dots. If the cavity

did not have separate modes near the exciton and biexciton doublet frequencies, then only one transition could couple strongly to the cavity, and the other transition would be sufficiently off resonance ($\delta > q$) such that the Purcell effect for this frequency would be suppressed, i.e., either the biexciton-exciton or exciton-ground transitions may be well coupled to the cavity, but not both.

It may be possible to engineer a small cavity with a pair of closely spaced modes using photonic crystals. If during the growth of each DBR stack, one layer was permitted to grow to larger than $\lambda/4$, then the cavity would look more like two coupled cavities, which may have the desired split modes. Certainly, geometric effects in micropillars have been shown to produce a pair of modes spaced by ~ 5 meV,[30] though this was due to lifting polarization degeneracy with elliptical cross-section cavities, which is undesirable for our scheme.

Experiments using hemispherical cavities, consisting of a planar Bragg reflector at the focal plane of a hemispherical reflector, of length 50–1000 μm are currently underway for quantum information processing purposes.[24] In this configuration, the cavity mode waist diameter is of comparable size to the optical wavelength and coincident with a quantum dot so that the exciton-cavity mode coupling strength is reasonably large. This arrangement may provide the two requirements of the present paper: both strong coupling between the dot excitations and the cavity mode (up to several tens of μeV) and small FSR so that each doublet is on resonance with a nearby mode. It is quite plausible that by tuning the cavity length to vary the FSR and applying an external dc electric field to induce a Stark shift in the doublet frequencies, one may bring both doublets close to cavity modes simultaneously, as depicted in Fig. 1(b), thereby realising the requirements of this proposal.

VIII. SUMMARY

We have shown analytically that by using a cavity with a particular mode structure facilitates the production of polarization-entangled photon pairs from an asymmetric quantum dot, which otherwise produces photon pairs entangled in both polarization and frequency. We demonstrated this by computing the visibility of two-photon interference fringes produced using photons generated from such a cavity-quantum dot structure, and related this to their potential to demonstrate Bell-inequality violations.

We have quantified the effect of various errors in the cavity mode structure, showing that the visibility is not degraded badly by mistuned cavities or unbalanced dipole coupling strengths, and for experimentally accessible regimes is above the threshold at which Bell-inequality violations may be detected.

Of major significance to this scheme is the phase accumulated between single-photon emission events. By defining the phase-averaged visibility, we were able to compute the effect of ignoring this phase on Bell-inequality and two-photon visibility measurements. Such phase ignorance arises when the available time resolution of the photon detection apparatus is longer than the asymmetry splitting, Δ.

We showed that ignoring the phase reduces the effective entanglement, but there are still experimentally accessible regions of parameter space that exhibit Bell-inequality violation, even when the phase is ignored, and the two-photon states are thus potentially useful sources of entanglement.

ACKNOWLEDGMENTS

We would like to thank Andrew Shields and Mark Stevenson who prompted this work, and for their helpful discussions and comments. We would also like to thank Sean Barrett and Michael Raymer for useful conversations and suggestions. T.M.S. thanks the Hackett Scholarships Committee and CVCP for financial support. G.J.M. acknowledges financial support from the CMI. C.H.W.B. thanks the EPSRC for financial support.

*Electronic address: tms29@cam.ac.uk

[1] M. A. Nielsen and I. L. Chuang, *Quantum Computation and Quantum Information* (Cambridge University Press, Cambridge, 2000).

[2] N. Gisin, G.G. Ribordy, W. Tittel, and H. Zbinden, Rev. Mod. Phys. **74**, 145 (2002).

[3] F. Knill, R. Laflamme, and G.J. Milburn, Nature (London) **409**, 46 (2001).

[4] Z.L. Yuan, B.E. Kardynal, R.M. Stevenson, A.J. Shields, C.J. Lobo, K. Cooper, N.S. Beattie, D.A. Ritchie, and M. Pepper, Science **295**, 102 (2002).

[5] A. J. Shields, R. M. Stevenson, R. M. Thompson, Z. Yuan, and B. E. Kardynal, in *Nano-Physics & Bio-Electronics: A New Odyssey*, edited by T. Chakraborty, F. Peeters, and U. Sivan (Elsevier, New York, 2002), Chap. 4.

[6] O. Benson, C. Santori, M. Pelton, and Y. Yamamoto, Phys. Rev. Lett. **84**, 2513 (2000).

[7] G. Chen, T.H. Stievater, E.T. Batteh, X. Li, D.-G. Steel, D. Gammon, D.S. Katzer, D. Park, and L.J. Sham, Phys. Rev. Lett. **88**, 117901 (2002).

[8] D. Gammon, E.S. Snow, B.V. Shanabrook, D.S. Katzer, and D. Park, Phys. Rev. Lett. **76**, 3005 (1996).

[9] S.V. Gupalov, E.L. Ivchenko, and A.V. Kavokin, JETP **86**, 388 (1998).

[10] V.D. Kulakovskii, G. Bacher, R. Weigand, T. Kümmell, A. Forchel, E. Borovitskaya, K. Leonardi, and D. Hommel, Phys. Rev. Lett. **82**, 1780 (1999).

[11] R.M. Stevenson, R.M. Thompson, A.J. Shields, I. Farrer, B.E. Kardynal, D.A. Ritchie, and M. Pepper, Phys. Rev. B **66**, 081302 (2002).

[12] D. Branning, W.P. Grice, R. Erdmann, and I.A. Walmsley, Phys. Rev. Lett. **83**, 955 (1999).

[13] K. Banaszek, A.B. U'Ren, and I.A. Walmsley, quant-ph/0103026 (unpublished).

[14] Y. Yamamoto and A. Imamoğlu, *Mesoscopic Quantum Optics* (Wiley-Interscience, New York, 1999).

[15] L. Mandel and E. Wolf, *Optical Coherence and Quantum Optics* (Cambridge University Press, Cambridge, 1995).
[16] H. Wiseman, Ph.D. thesis, University of Queensland, 1994.
[17] C. W. Gardiner and P. Zoller, *Quantum Noise* (Springer, New York, 2000).
[18] K. Edamatsu, R. Shimizu, and T. Itoh, Phys. Rev. Lett. **89**, 213601 (2002).
[19] A. Ekert and P. Horodecki, quant-ph/0111064 (unpublished).
[20] H.M. Wiseman and G.J. Milburn, Phys. Rev. A **47**, 1652 (1993).
[21] D. F. Walls and G. J. Milburn, *Quantum Optics* (Springer-Verlag, Berlin, 1994).
[22] T. Flissikowski, A. Hundt, M. Lowisch, M. Rabe, and F. Henneberger, Phys. Rev. Lett. **86**, 3172 (2001).
[23] A. Imamoğlu, D.D. Awschalom, G. Burkard, D.P. DiVincenzo, D. Loss, M. Sherwin, and A. Small, Phys. Rev. Lett. **83**, 4204 (1999).
[24] M. Raymer (private communication).
[25] M. Pelton, C. Santori, J. Vučković, B. Zhang, G.S. Solomon, J. Plant, and Y. Yamamoto, Phys. Rev. Lett. **89**, 233602 (2002).
[26] J.M. Gérard, B. Sermage, B. Gayral, B. Legrand, E. Costard, and V. Thierry-Mieg, Phys. Rev. Lett. **81**, 1110 (1998).
[27] D. Birkedal, K. Leosson, and J.M. Hvam, Phys. Rev. Lett. **87**, 227401 (2001).
[28] P. Borri, W. Langbein, J.M. Hvam, and F. Martelli, Phys. Rev. B **60**, 4505 (1999).
[29] H. J. Kimble, in *Cavity Quantum Electrodynamics*, edited by P. R. Berman, Advances in Atomic, Molecular, and Optical Physics, Supplement 2 (Academic Press, San Diego, 1994).
[30] I. Robert, E. Moreau, J.M. Gerard, and I. Abram, J. Lumin. **94-95**, 798 (2001).